

## Virtual energy storage gain resulting from the spatio-temporal coordination of hydropower over Europe

Anders Wörman<sup>a,\*</sup>, Cintia Bertacchi Uvo<sup>b</sup>, Luigia Brandimarte<sup>a</sup>, Stefan Busse<sup>c</sup>, Louise Crochemore<sup>d</sup>, Marc Girons Lopez<sup>d</sup>, Shuang Hao<sup>a</sup>, Ilias Pechlivanidis<sup>d</sup>, Joakim Riml<sup>a</sup>

<sup>a</sup> KTH – Royal Institute of Technology, 100 44 Stockholm, Sweden

<sup>b</sup> Lund University, Lund, Sweden

<sup>c</sup> Uniper AB, Sundsvall, Sweden

<sup>d</sup> Swedish Meteorological and Hydrological Institute, Norrköping, Sweden

### HIGHLIGHTS

- Virtual energy storage gain results from spatio-temporal coordination of hydropower.
- Climate-driven fluctuations in renewable energy can be compensated by virtual energy storage.
- Virtual energy storage is twice the storage capacity of hydropower reservoirs in Europe.
- A new spectral method was developed for analysis of energy storage gain.

### ARTICLE INFO

#### Keywords:

Virtual energy storage  
Climate fluctuations  
Spatio-temporal coordination of hydropower  
Spectral analysis  
Energy balance

### ABSTRACT

The viability of a renewable electricity system depends on a relatively small share of hydropower storage resources to regulate climate variations and the spatially uneven distribution of renewable energy. By spatio-temporal coordination of hydropower production over larger regions, the energy storage demand will be reduced and contribute to a “virtual” energy storage gain that in Europe was found to be almost twice the actual energy storage capacity of hydropower reservoirs. In an attempt to quantify this gain, hydropower availability was simulated for most parts of the European continent for a 35-year period based on historical hydro-meteorological data. The most significant benefits from spatio-temporal management arise at distances between 1200 and 3000 km, i.e., on the continental scale, which can have implications for a future renewable energy system at large. Furthermore, we discuss a condition termed “energy-domain-specific drought”, which is a risk that can be reduced by the spatio-temporal management of power production. Virtual energy storage gain is not explicitly considered in the management models of hydropower production systems but could in principle complement existing management incentives.

### 1. Introduction

On average, there are sufficient renewable energy resources available on Earth to fulfil human demand for electricity and energy in general ([Appendix A](#)). This led the International Energy Agency (IEA) in its 2016 World Energy Outlook (WEO) to state, “The technical potential for renewable energy is enormous and the resources available around the world could, in theory, meet all the energy needs projected in each WEO scenario with ease.” However, availability and access to energy sources alone do not guarantee viable and stable renewable electricity systems. Several factors, such as long-term climate variations, the

spatially uneven distribution of energy sources and constraints due to energy storage, transmission and maximum power capacities, contribute to making the renewable energy system an intertwined issue [[1,2](#)]. Therefore, there is a need for long-term energy utilization forecasts to support production planning, technical solutions and power regulation. Hydropower represents a relatively small share of the full renewable energy potential [[3–5](#)], and its potential is only approximately 9% of the total energy demand ([Appendix A](#)). However, it offers important hydro-energy storage that can be used to regulate the intermittent nature of renewable energy sources as well as seasonal variation in energy demand and general balancing of the electrical grid. In

\* Corresponding author.

E-mail address: [worman@kth.se](mailto:worman@kth.se) (A. Wörman).

this sense, the analysis of historical hydrometeorological data may offer important insight into the complex connections between energy storage, the intermittent and spatially heterogeneous availability of hydropower, the spatial transmission capacity and the suitable management of electricity production.

Management or optimization models for multiple hydropower stations are normally defined for individual river basins [6–9]. This implies a regional sub-optimization of production that in general does not lead to global optimization of production, but production management is coupled through economic incentives over a larger energy market [10]. However, the coordination of hydropower production over long distances can specifically result in smaller variance in the instantaneous power availability on a global-scale system. This leads to a reduced combined need for energy storage to overcome periods of low energy availability, periods that can be regarded as “energy droughts” [11]. For example, the variance in the water flow summed from two (hypothetically) equal river basins can vary from zero to four times the variance in the individual flows depending on the covariation of flows from the two basins. By considering this covariation of flows in hydropower production management – spatio-temporally coordinating the production – energy storage demand can potentially be reduced. Such a reduction in energy storage demand can be seen as a virtual energy storage gain. In addition to energy droughts, another consequence of the lack of coordination in power production can be the direct spillage of water at individual hydropower plants and the loss of total production. Incentives for virtual energy storage gain and reduced probability for energy droughts in a global optimization context are not yet explicitly considered in hydropower management models [7] but could in principle be acknowledged based on appropriate information. Moreover, co-fluctuations in both space and time between runoff and other renewable energy sources have been identified as a key problem for handling a future intermittent climate-related energy system [12].

Climate-driven fluctuations in renewable energy availability can be substantial in magnitude with large spatial covariation over continents. For Europe, Kingston et al. [13,14] showed how increasing North Atlantic Oscillation (NAO) and Arctic Oscillation (AO) are connected to increasing streamflow over Northern Europe. In contrast, Trigo et al. [15] showed that increases in water resource availability in the Iberian Peninsula are negatively correlated with the NAO. Brandimarte et al. [16] analysed the interdependence between the NAO and winter precipitation, river flow and temperature in the Mediterranean, finding that the area is mostly negatively correlated with the NAO. Bartoli et al. [17] found a bi-annual variability of winter precipitation in the European Alps, while similar bi-annual variation in precipitation was found in Scandinavia [18,19]. Furthermore, changes in precipitation and temperature at the seasonal scale over Sweden have been shown to be connected to the low-frequency variations in the Northern Hemisphere teleconnection patterns (e.g., [20,21]). Such frequency decomposition of the hydropower availability in Sweden and climate indices as well as other renewable energies, such as wind and solar intensity, shows that especially strong climate-driven correlations exist over periods of 2, 3.6 and 8 years [21,22]. These long-term climate-driven fluctuations in renewable energy have direct importance for the management of renewable energy systems, energy transmission and energy storage [23,2]. However, those fluctuations also have strong impacts on other aspects of society, such as river floods [24] and droughts, with subsequent effects on local economies through effects on, e.g., agriculture and other sub-economies [25,26], which feeds back on the energy demand.

Consequently, an improved understanding of the spatio-temporal distribution of renewable energy is of key importance. The significant climate-driven covariation of renewable energy that has been observed over large regions is important for regional production coordination and reduced energy storage demand, as well as for defining economic incentives in management models supporting production management. Moreover, climate-driven fluctuations in hydropower availability

appear on a wide spectrum of frequencies as shown by Wörman et al. [19] that explored frequencies of variation of the hydropower availability, and Foster [27] and Uvo et al. [28] that analyzed the variability of river discharge and water availability in connection to climate variability. Hence, there is a need for a spectral theory that relates energy storage need to the considered frequency range of variations in hydropower availability.

The overall aim of this study is to provide a basic statistical analysis of spatio-temporal variability in hydropower availability over the European continent and to analyse the connection of such variability with energy storage demand over the range of relevant frequencies as seen in historical, multidecadal hydrometeorological time-series. This includes determining the potential reduction in the energy storage demand from spatio-temporally coordinating hydropower production on the continental scale. To cover a large geographical domain, this investigation is based on modelled runoff from tens of thousands of European watersheds, which is based on extensive and reliable geographical and hydrometeorological data. The associated potential for hydro-energy is estimated both as the full landscape potential for runoff and as the production capacity of a large part of the existing hydropower system in Europe. An important question this paper aims to address is *“How can the spatio-temporal coordination of hydropower production reduce the effects of climate-driven variance in the total production and, hence, reduce energy storage demands due to climate fluctuations?”*. Since climate-driven fluctuations in runoff occur over a range of different frequencies [18,27,28], a spectral correlation analysis will facilitate analysis of the return periods of energy droughts. To the authors’ knowledge, such an analysis has never been conducted for the hydropower system at the European scale.

## 2. Data and study region

The daily runoff for a 35-year period (1981–2015) is produced for 35,408 watersheds covering Europe and parts of the Middle East. The data are produced using the European setup of the HYPE hydrological model (Hydrological Prediction for the Environment; [29], known as E-HYPE [30,31] (Fig. 1). E-HYPE is a distributed process-based model with a median resolution of 215 km<sup>2</sup> that aims to provide a wide range of hydrologic variables (e.g., snow, evapotranspiration, runoff, reservoir regulation, irrigation management) while ensuring optimal runoff simulations over Europe. The model setup relies on openly available landscape elevation, river network, irrigation, soil and land cover datasets. The model was calibrated on a set of 115 European watersheds chosen as representative of the diversity of climate, soil, land use and main human impacts over Europe [31] against runoff observations from the Global Runoff Data Centre (GRDC) Reference Dataset (<http://www.bafg.de/GRDC/>). Here, E-HYPE was forced with precipitation and temperature from HydroGFD (Hydrological Global Forcing Data; [32]; available at a 0.5 × 0.5° resolution) based on the grid cell nearest to each watershed centroid.

The total area of the simulation domain is 8.74 × 10<sup>6</sup> km<sup>2</sup> compared to the reported area of European countries, which is 10.18 × 10<sup>6</sup> km<sup>2</sup>. The smallest watershed of E-HYPE’s 35,408 sub-watersheds is 0.58 m<sup>2</sup>, the maximum is 1.79 × 10<sup>4</sup> km<sup>2</sup>, and the mean is 2.46 × 10<sup>2</sup> km<sup>2</sup>. The volumetric mean runoff was 91,094 m<sup>3</sup>/s over the entire domain, which is the runoff to surface water without consideration of evaporation further downstream, such as from lakes and reservoirs. The hydropower potential was simulated for the 3032 main river basins, i.e., watersheds with effluence to the sea. Due to this definition of main river basins, the model domain includes a very large range of watershed areas, as seen in the statistics provided in Table 1, from small areas close to the sea up to continental river basins. Data on the hydropower system of Europe were taken from the Global Reservoir and Dam Database (GRanD, <http://globaldamwatch.org/grand/>) that accounts for all dams and reservoirs with a storage capacity of more than 0.1 km<sup>3</sup> [33,34], which included 1377 hydropower stations within the E-HYPE

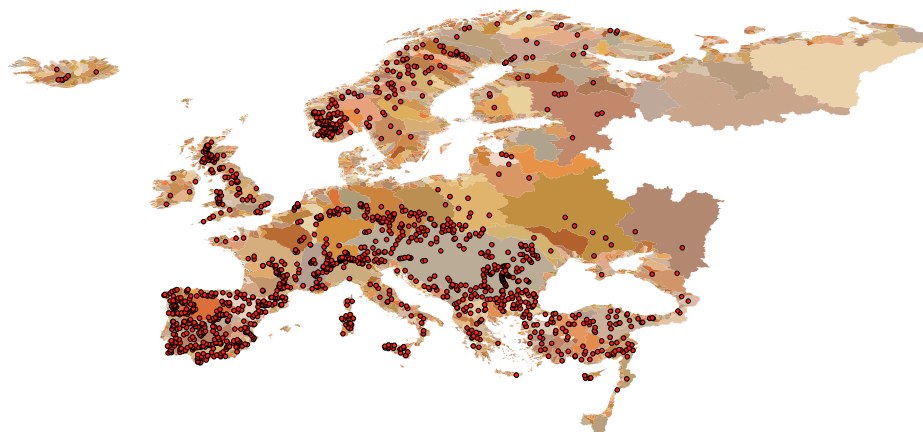


**Fig. 1.** Map of the 3032 main watersheds with effluence to the sea included in the E-HYPE study area and the 1377 hydropower stations (brown dots) and associated reservoirs that are found in the GranD database.

model domain distributed in 326 main river basins. This database is considered state-of-the-art, yet it is incomplete in terms of reservoir volume and, especially, the number of power plant sites and full data for each site. Nevertheless, this database is used as an extensive characterization of the hydropower system in all watersheds covered by the E-HYPE model domain (Fig. 1).

### 3. Analytical methods

The approach taken in this study is to analyse historical modelled runoff from a large number of watersheds covering Europe to assess the spatio-temporal production potential at a large number of the most important hydropower plants (Sections 3.1 and 3.2). In addition, a formulation based on the energy balance was derived for the variance in the potential production time-series at those plants with consideration of the energy storage in hydropower reservoirs (Section 3.3). This analysis is applied to the historical runoff data and will minimize the total production variance at the GranD hydropower stations within a certain “coordination distance” by acknowledging the covariation in potential production at those stations. Finally, a spectral approach is developed that relates the variance of potential production to the energy storage demand of the considered set of hydropower stations as a function of the considered frequencies of variation (Section 3.4).

#### 3.1. Hydropower potential

The time-series of the potential energy of runoff was calculated based on a) the landscape elevation following the approach proposed by Wörman et al. [19] (hereafter named landscape hydropower potential) and b) the energy production capacity at the specific hydropower plant sites included in the GranD database. The areal density of the potential power of the runoff in sub-watershed  $i$  relative to the sea level can be expressed as follows:

$$\frac{dP_{r,i}(x, y, t)}{dA} = \rho g h_i(x, y) q_i(t) \quad (1)$$

where  $P_r$  is the (landscape potential of the) power of runoff (J/s),  $A$  is the area defining the runoff simulation ( $\text{m}^2$ ),  $q = dQ/dA$  is the runoff per area ( $\text{m}^3/(\text{m}^2 \text{s})$ ),  $Q$  is the volumetric runoff ( $\text{m}^3/\text{s}$ ),  $\rho$  is the density of water ( $\text{kg/m}^3$ ),  $g$  is the acceleration due to gravity ( $\text{m/s}^2$ ), and  $h$  is the landscape elevation above sea level (m). The integration of power for the main areas was based on the areas associated with the 35,408 sub-watersheds, but the result was aggregated on the 3032 main river basins. The potential hydropower production, denoted  $P_c$ , was estimated at plant locations included in the GranD database in a similar way for all the main watersheds based on their entire upstream area, the average runoff of that area and the fall height at the different sites as approximated by the dam height. This means that all possible water spillage and electric generation limitations of the turbines were neglected.

The production system defined in the GranD data dated 19/03/2019 was approximated (by taking the dam height as the hydraulic head over the hydropower plant and upstream area as well as runoff from the E-HYPE simulations) to cover a potential production capacity of approximately 366 TWh/y in the entire E-HYPE domain. The statistics of the power potential of the main river basins are provided in Table 1. Within the EU-28 countries, this capacity was found to be 200 TWh/y compared with the actual hydropower production of 331 TWh/y during 2017 according to the International Energy Agency (IEA). The covered energy storage capacity in the reservoirs included in GranD can be estimated to be 81,000 GWh compared with the 183,000 GWh reported as the energy storage capacity of most European countries except Russia [35]. The proportion between the production capacity and energy storage is believed to be representative with sufficient accuracy for the study objectives.

#### 3.2. Energy balance statement of a delimited geographical-technical domain

The balance of power production and consumption has to be satisfied over a single, unified technical electricity system with common boundaries as long as energy export and import are not considered. However, by introducing energy flows through system boundaries and

**Table 1**

Statistics of the 3032 main river basins, including the GranD data distribution on these river basins. There are 325 main river basins with hydropower production and 2707 without hydropower production.

	Sum (A)	Mean value, $\mu_A$	Standard deviation, $\sigma_A$	Min (A)	Max (A)
Watershed area [ $\text{m}^2$ ]	$8.74 \times 10^{12}$	$2.88 \times 10^9$	$23.2 \times 10^9$	$1.0 \times 10^6$	$0.798 \times 10^{12}$
Landscape potential [TWh/y]	3569	1.18	10.8	$\approx 0$	487
Potential at GranD stations [TWh/y]	366	0.12	1.92	0	65.4

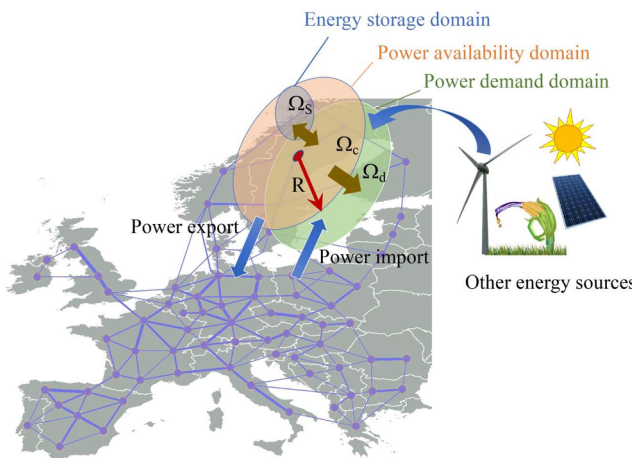


**Fig. 2.** Definition sketch for storage, production and demand regions, various energy fluxes in relation to these system delimitations and coordination distance ( $R$ ). The symbol  $\Omega$  denotes domains for storage, production capacity and demand of energy. Brown arrows denote internal energy fluxes between these domains, and blue arrows denote external energy fluxes.

different areas for production and consumption, one can schematically define the energy balance in the form of:

$$\frac{\partial E(t)}{\partial t} \Big|_{\Omega_s} = (P_c(t) - X(t))|_{\Omega_c} - (P_d(t) - I(t) - e(t))|_{\Omega_d} \quad (2)$$

where  $E$  = energy storage (J),  $P_c$  = power availability or production capacity (W),  $P_d$  = power demand or consumption (W),  $X$  = power export from the production domain (W),  $I$  = power import to the consumption domain (W),  $e$  = power from other energy sources (W),  $t$  = time (s), and  $\Omega$  denote the delimited domains for storage, production and demand (Fig. 2). The domains for production capacity,  $\Omega_c$ , and consumption or demand,  $\Omega_d$ , are generally not delimited (bounded) in the same way, which is why an important problem in electrical power system planning is to connect the production and demand with an appropriate power grid. In fact, by selecting different regions for energy storage, power availability capacity and power demand, one indirectly defines conditions for export and import in the power grid as well as the fluxes between production and consumption domains (Fig. 2). The latter fluxes can be regarded as “internal” with respect to the energy balance, Eq. (2), where the union of  $\Omega_s$ ,  $\Omega_c$  and  $\Omega_d$  form a conceptually common domain, but which can be geographically fragmented. Furthermore, in this study, a “rest power” is defined by the introduction of the auxiliary rest term

$$\varepsilon = -X|_{\Omega_c} - (P_d - I - e)|_{\Omega_d} \quad (3)$$

The definition of this rest term is important since it can also be seen as an imbalance in production capacity and storage, hence offering interpretation of how to technically deal with such imbalances. A positive imbalance between production capacity and storage within the domain  $\Omega$  should match the energy demand, but can also be compensated by export of energy, whereas a negative imbalance can be compensated by import of energy or utilization of other energy sources. In the subsequent analysis of the energy balance, a conceptually common domain  $\Omega$  is applied for both energy storage and production. In practice, such energy balance over a common domain is generally applied in cases when a single grand reservoir regulates the discharge to several downstream “cascading” hydropower plants. However, the application of the same assumption for energy flows across the water divides of river basins implies that one assumes unlimited transmission capacity of the electrical grid to support such energy production coordination. Furthermore, it will be assumed that power plants have infinite power capacity and there is no spillage and no temporal energy storage restrictions at individual sites. These simplifications will, however, be

further restricted by acknowledging spatio-temporal coordination only within a “coordination distance” within the domain (see below).

Consequently, Eqs. (2) and (3) yield an energy balance statement in the form of

$$\left( \frac{\partial E}{\partial t} - P_c \right) \Big|_{\Omega} = \varepsilon \quad (4)$$

Specifically, the simulated runoff time-series were generated by E-HYPE in 35,408 sub-watersheds, but aggregated for the 3032 main river basins (with an outlet to the sea or ocean) accounted for in these simulations, of which 326 river basins contain grand dams and possess hydropower plants. Since the regulatory capacity may not fully balance the production availability capacity in each of the 326 major river basins that contain hydropower plants, this domain definition implies that production and regulatory capacities are shared between the main river basins within the common domain  $\Omega$  through the coordination of power production transmission in the electrical grid. Consequently, from a statement such as Eq. (4), one can interpret the total energy storage demand  $\Delta E$  as an integration over a time period  $\Delta T$ , i.e.,  $\Delta E = \int_{\Delta T} ((P_c)|_{\Omega} + \varepsilon) dt$ . From this expression, one can see that an imbalance between the energy production capacity and energy storage demand can be compensated by power export or import, fluctuations in energy demand or production coordination using other energy sources (Eq. (3)). However, for the assessment of the virtual storage gain within hydropower, the rest power term  $\varepsilon$  will be taken as a constant that is balanced by a constant hydropower production  $\bar{P}_c$ , i.e.,  $\varepsilon = -\bar{P}_c$ . The energy balance Eq. (4) can then be given in the form of the fluctuating properties  $E'$  and  $P_c'$  as

$$\left( \frac{\partial E'}{\partial t} - P_c' \right) \Big|_{\Omega} = 0 \quad (5)$$

where  $\dot{P}_c(t) = P_c(t) - \bar{P}_c$ ,  $\bar{P}_c$  = the temporally expected value of  $P_c$ ,  $E'(t) = E(t) - \bar{E}$ , and  $\bar{E}$  = the temporally expected value of  $E$ . This is a special case of energy system management by which fluctuations in hydropower availability are completely balanced by hydropower storage within the domain  $\Omega$ . For practical purposes, one could assume a constant storage demand  $\bar{E} = 0$ , which is why  $E'$  can be seen as the real energy storage demand. From this expression, one can interpret an available energy storage capacity less than the demand,  $\Delta E_{av} < \Delta E = \int_{\Delta T} ((P_c')|_{\Omega}) dt$ , as an *energy drought* specific to the considered energy source and the delimitation of the domain  $\Omega$  shown in Fig. 2, which will be referred to as *energy-domain-specific drought*. In practice, energy production management generally acknowledges a rest power term that varies over time and an economic forecast model that represents a spatial coordination of the production. The economic model reflects a common (uniform) market behaviour [7,18], but such common management incentives do not necessarily consider minimization of the energy storage demand,  $\int_{\Delta T} ((P_c')|_{\Omega}) dt$ , or risks for energy droughts.

### 3.3. Estimates of variance in power and energy storage

It can be shown from  $(\partial E'/\partial t - P_c')|_{\Omega} = 0$  that if the power availability capacity  $P_c$  follows a single harmonic function, the demanded maximum energy storage  $E_{max}$  (J) is expressed as

$$E_{max} = \sqrt{2} Std(P_c)T/\pi \quad (6)$$

where  $f = 1/T$ ,  $f$  = frequency ( $s^{-1}$ ) and  $T$  = period (s). It follows from this simple result that both the standard deviation in the power availability and the period of fluctuation are important for the maximum energy storage demand. Moreover, the total variance of the sum of power time-series availability can be calculated for all watersheds within the analysed domain  $\Omega$ , which are separated (or lagged) by a separation distance  $r$ . These separation distances were based on the Euclidean distances between pairwise watershed centroids  $(x_i, y_i)$  and  $(x_j, y_j)$  of the

aggregated areas that fulfil  $r_{i,j} < R$ , where  $i$  and  $j$  are indices for watersheds (main river basins) located within the analysed domain  $\Omega$ , and  $R$  is the maximum coordination distance considered in the hydropower system (Fig. 2). The total variance of the sum of all individual time-series of the power availability capacity within the considered domain can be expressed as:

$$\text{Var}\left(\sum_{i=1}^N P_{c,i}\right) \Big|_{r < R} = \sum_{i=1}^N \text{Var}(P_{c,i}) + \sum_{i \neq j}^N \text{Cov}(P_{c,i}; P_{c,j}) \quad (7)$$

where  $N$  = number of watersheds considered within the analysed domain  $\Omega$ , and  $i$  and  $j$  are sub-watershed indices. The second summation on the right-hand side of Eq. (7) represents the covariance of the production capacities in different sub-watersheds. Occasionally, with high separation distances between the watershed centroids  $i$  and  $j$ , this term can be negative and hence contribute to reducing the variance of the sum of the power time-series and significantly decreasing the storage need. However, generally for shorter separation distances, the covariance terms are positive contributions that are bounded by a maximum variance obtained when the time-series are perfectly correlated. At all locations within the coordination distance  $R$ , the variance in the power time-series was calculated by accounting for their covariance according to Eq. (7).

The variance of the sum of completely uncorrelated power time-series can be expressed as  $\text{Var}(\sum_{i=1}^N P_{c,i}) = \sum_{i=1}^N \text{Var}(P_{c,i})$ . This means that the standard deviation of the sum of uncorrelated power time-series  $\text{Std}(\sum_{i=1}^N P_{c,i}) = \sqrt{\sum_{i=1}^N \text{Var}(P_{c,i})}$ , which is generally much smaller than the sum of the standard deviation of independent power time-series,  $\sum_{i=1}^N \text{Std}(P_{c,i})$ . Since the total (of all sub-watersheds) energy storage demand  $E \propto \sum_{i=1}^N \text{Std}(P_{c,i})$ , a fully independent management of the sub-watersheds, i.e., when  $R < r$ , implies a 100% correlation between the time-series and that the variance in the power time-series takes the following form:

$$\text{Var}\left(\sum_{i=1}^N P_{c,i}\right) \Big|_{R < r} = \sum_{i=1}^N \text{Var}(P_{c,i}) + \sum_{i \neq j}^N \text{Std}(P_{c,i})\text{Std}(P_{c,j}) \quad (8)$$

Eq. (8) assumes a 100% correlation between the time-series and implies that  $E \propto \sum_{i=1}^N \text{Std}(P_{c,i}) = \sqrt{\text{Var}(\sum_{i=1}^N P_{c,i})} \Big|_{R < r}$ . This means that the variance in power availability within the coordination distance  $R$  is smaller than that at longer distances, i.e., that  $\text{Var}(\sum_{i=1}^N P_{c,i}) \Big|_{r < R} \leq \text{Var}(\sum_{i=1}^N P_{c,i}) \Big|_{r > R}$ , where the left and right-hand sides are determined from Eqs. (7) and (8), respectively. Consequently, there will inevitably be lower variance in the power production due to spatio-temporal coordination at distances  $r < R$  compared to that without such coordination at distances  $R < r$ .

### 3.4. Spectral correlation analysis

To facilitate the analysis of the variance in hydro-energy availability, the energy time-series were transformed into their spectral correspondences, which is fundamentally the variance in the time-series distributed on the frequency (or period). This is useful since, as mentioned, the standard deviation of the required energy storage (in Joules) is directly proportional to the standard deviation of the power availability capacity (in Watts) and the period of variability,  $\sum_{i=1}^N E_i \propto \sum_{i=1}^N T_i \text{Std}(P_{c,i})$ . Hence, spectral decomposition of the power time-series offers a formal way of dividing the storage need on climate periods  $T$  (or frequency  $f$ ). Specifically, the energy balance  $\partial E / \partial t - \sum_{i=1}^N P_{c,i} = 0$  can be expressed on a spectral form as  $(2\pi f)^2 S(E(f)) = S(\sum_{i=1}^N P_{c,i}(f))$ , where  $S$  is the power spectral density operator and  $E(f)$  is the total energy storage demand over the entire domain  $\Omega$  associated with the frequency  $f$ . The variance of the total storage can be obtained by integration of the storage spectrum

$$\text{Var}(E) = 2 \int_{f_1}^{f_2} S(E(f)) df = 2 \int_{f_1}^{f_2} \frac{S(\sum_{i=1}^N P_{c,i})}{(2\pi f)^2} df \quad (9)$$

Moreover, the maximum energy storage demand is given by  $E_{max} = \sqrt{a\text{Var}(E)}$ , where  $a$  (-) is a coefficient that depends on the distribution of  $E$  [36]. For a uniform distribution,  $a = 12$ , but for a single harmonic function,  $a = 2$ , which is the “conservative” value adopted in the discussion of the results. Similarly, the total variance in the time-series of the power availability capacity becomes

$$\text{Var}\left(\sum_{i=1}^N P_{c,i}\right) = 2 \int_{f_1}^{f_2} S(\sum_{i=1}^N P_{c,i}) df \quad (10)$$

As the coordination distance  $R$  varies, the assessment of these spectra over the range of all possible watershed combinations  $(i,j)$  can be quite computationally heavy when repeated for different combinations of sub-watersheds, which motivated the use of the following relationship for  $N$  watersheds within the coordination distance:

$$S(\sum_{i=1}^N P_{c,i}) = \left( \sum_{i=1}^N S(P_{c,i}) + \sum_{i \neq j}^N \text{Re}\{S(P_{c,i}; P_{c,j})\} \right) \quad (11)$$

where  $\text{Re}$  denotes the real part and the second term is the covariance spectral density function. The total number of possible interactions between the 3032 main river basins considered in the analysis of the covariance spectra was up to  $9.18 \times 10^6$  as the coordination distance approaches its maximum 89.18 DD. Eq. (11) can be seen as the discrete form of the auto-covariance spectral density function, where the summation is analogous to the integration over the correlation distance of the auto-covariance spectral density function. To reduce the computational requirements of the large number of covariance spectra, the daily power time-series was first averaged in 10-day stepwise moving windows so that the original time-series with 12,752 data points was reduced to 1275 data points. The latter sparse time-series were detrended and filtered using Hamming windowing on the entire time-series. Finally, the spectral analysis was conducted using Welch's method as implemented in the CPSD-function of MATLAB®, which includes an additional segment-wise filtration. Frequencies are distributed over 256 unisized frequency steps from zero to half the data frequency ( $0.05 \text{ days}^{-1}$ ), which leads to a nonuniform distribution of period steps. The longest time period considered in these analyses was that of the zero frequency, but the second longest was 14.027 years, which is the longest period considered within the 35-year-long data record.

## 4. Results

### 4.1. Climate-driven variance of hydropower availability

On average, the total power of runoff given by the landscape elevation – the landscape hydropower potential,  $P_r$  – was found to be 3569 TWh/y for the domain covered in the analysis (Fig. 1), whereas as mentioned, the power associated with the production system defined in the GranD database is approximately only 366 TWh/y. The temporal variation in the spatial average of  $P_r(t)$  as a simultaneous time-series for all of Europe is shown in Fig. 3. Some properties of the landscape hydropower potential are given in Table 2 in which it is seen that the standard deviation in the daily power is 1231 TWh/y, whereas the moving annual average has a standard deviation of 248 TWh/y. Despite a significant decrease in the standard deviation of the power availability with an increasing moving-averaging window  $T_w$ , Eq. (6) indicates that the associated energy storage demand still increases significantly with  $T_w$ . These approximate differences in energy storage demand at different periods will be used for comparison with the results from the spectral approach, whereby the energy storage demand is considered simultaneously at all periods.

The power spectrum of the sum of the landscape hydropower potential for the whole domain (left-hand side of Eq. (10)) shows a clear annual peak, a weak bi-annual peak, a minimum of approximately 3.6 years and a less prominent longer-term (approximately 8–11 years) shallow peak (Fig. 4, left-hand side panel). This is consistent with what has been found previously for climate systems in Europe [37–41,19]. It

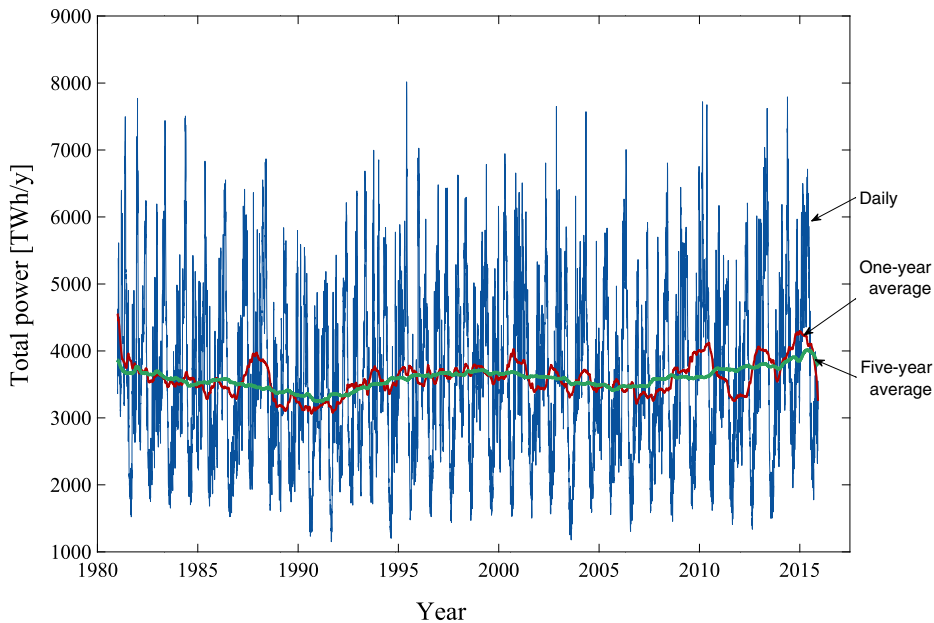


**Fig. 3.** Daily data of the landscape hydropower potential as a spatial average over 35,408 watersheds of Europe subject to runoff modelling using E-HYPE (blue curve). Red and green curves show moving averages in one- and five-year windows, respectively.

**Table 2**

Calculation of maximum energy storage demand based on the moving average time-series of the simultaneous landscape hydropower potential as shown in Fig. 3 (see Section 2.2). The maximum storage demand  $E_{max}$  is calculated from a harmonic function analogue to the simultaneous power time-series (third column of Table 2), which is used for comparison with the results from the spectral approach.

Moving average window, $T_w$ [y], used to smooth $\sum_{i=1}^N P_{c,i}$	$Std(\sum_{i=1}^N P_{c,i})$ [TWh/y]	$E_{max} = \sqrt{2} \frac{Std(\sum_{i=1}^N P_{c,i}) T_w}{\pi}$ [TWh]
1/365 (daily data)	1231	1.52
1	248	112
2	199	179
4.67	152	319
14	75	472

should be noted that since hydroclimatological time-series often show negative correlation, spectrum peaks in one variable can be manifested as minimums in another (i.e., temperature vs. precipitation). Local variations from this general pattern of the landscape hydropower potential over Europe generally arise, as demonstrated by the power spectrum on the right-hand side panel of Fig. 4. Appendix B more

thoroughly demonstrates the spatial variation in the power spectral diagrams over Europe.

The spectral estimate of the standard deviation of the landscape potential hydropower time-series goes from 3085 TWh/y without spatio-temporal coordination at  $R = 0$  DD (100% correlation between the time-series; using Eqs. (8), (10) and (11)) to 1149 TWh/y at full coordination at  $R = 89$  DD (using Eqs. (8), (10) and (11)) (Fig. 5). Within latitudes 45°N to 67°N, one decimal degree (DD) corresponds to between 78.7 and 43.50 km (the domain stretches from approximately 35°N to 70°N). This case represented by the red curve in Fig. 5 accounts for all time periods up to 14 years, but similar trends are found for a lower cut-off for the upper time period taken into consideration (black curves). The decay of the standard deviation in the power time-series with coordination distance  $R$  occurs because the variance calculation considers the covariation between the power time-series between sub-watersheds (Eq. (7)), which reduces the total variance when the separation distance between watershed centroids is less than  $R$ . The results also show the theoretical bounds of the power time-series in terms of a) that the time-series of the watersheds are uncorrelated, i.e., the standard deviation calculated directly from the sum of the filtered time-series as the square root of  $Var(\sum_{i=1}^N P_{c,i})$  (lower dotted line in Fig. 5) and b) that the watersheds are managed independently (100% correlation), i.e., the standard deviation is calculated from the right-hand

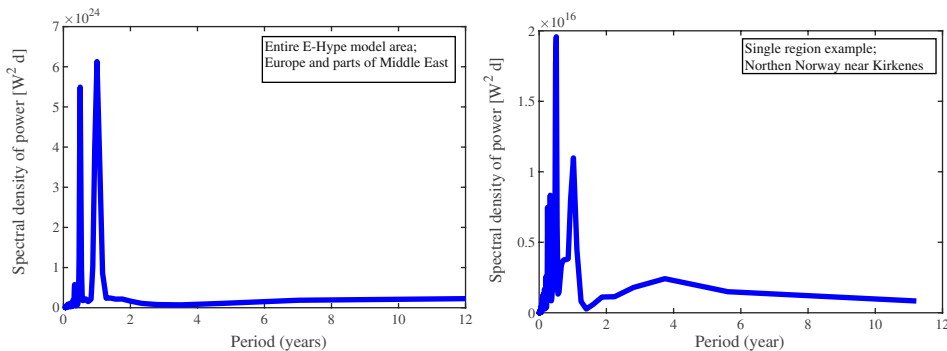


**Fig. 4.** Power spectral density of the landscape hydropower potential as a sum of time-series for all of Europe (to the left) and as an example for a single watershed (to the right).

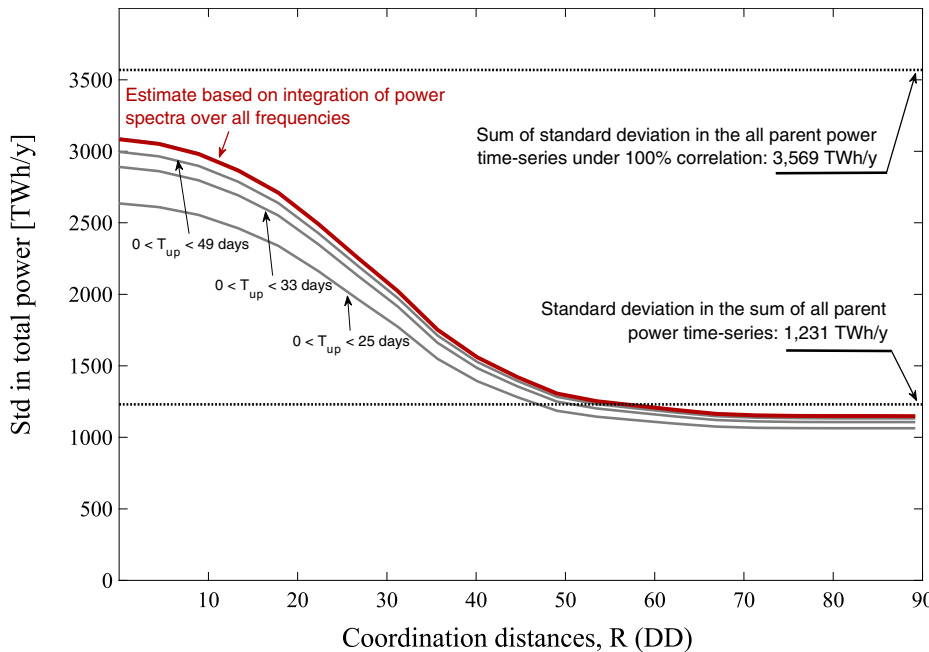


**Fig. 5.** Standard deviation of available hydropower for the period 1981 to 2015 in 3032 aggregated watersheds covering Europe and parts of the Middle East for all time periods up to 14 years (red curve) and for lower cut-offs of the time period taken into consideration (grey curves). The estimation is based on integration of the spectral density of hydropower, using Eqs. (1) and (2), by consideration of the covariation in hydropower availability existing up to a coordination distance, R. The standard deviation is consistently lower for both the completely non-coordinated ( $R = 0$ ) and the fully coordinated ( $R = 90$ ) cases compared to a direct variance estimate (dotted lines); Std-ratios are 0.60 and 0.66, respectively, which is similar as noted for individual areas (see Section 2.3).

side of Eq. (8) (upper, dotted line). Comparison of the spectral estimation with the direct variance estimations (dotted lines) shows a loss of standard deviation in the spectral transform procedure of 15% at  $R = 0$  and of 6.7% at  $R = 89$ . This leads to a slight underestimation of the power variations and possible energy storage gain from spatial coordination.

The highest change in gain with R in the form of reduced power variance due to spatio-temporal coordination is obtained as R goes from approximately 20 to 50 DD. Consequently, the most significant benefits in terms of lowering the power variance are obtained from spatial coordination on distances from approximately 1200 km up to 3000 km. The 10-day window allows assessment only from the lowest time period of 20 days, but the result still indicates that most of the standard deviation in the power is explained by periods below one month (see Fig. 5) by comparing the curves that were derived for different upper time periods  $T_{up}$ , where  $T_{up} = 1/f_1$  in the integration of Eq. (10).

#### 4.2. Energy storage demand due to landscape hydropower potential

By integrating  $S(E)$  over frequencies  $[f_1, f_2]$  according to Eq. (9), one obtains the maximum energy storage demand,  $E_{max}$ , associated with the landscape potential (Fig. 6). In Fig. 6, the upper period taken into consideration, as before, equals the lowest frequency acknowledged in the analysis, i.e.,  $T_{up} = 1/f_1$ . The standard deviation of the energy storage demand is highly sensitive to the upper period considered in the integration of  $S(E)$ , which is because the frequency appears in its second order in the denominator of  $S(P_{available})/f^2$ . Consequently, the ratio  $E_{max}|_{R=0}/E_{max}|_{R=89}$  is as high as 3.33 when all periods up to 14 years are considered, which corresponds to a maximum virtual energy storage gain, i.e., a reduction in the maximum energy storage demand associated with increasing coordination distance. For clarity, the maximum energy storage demand was derived as the square root of two times the standard deviation of the energy storage demand, which can be seen as a conservative (low) estimate of the demand. The maximum energy storage demand with increasing coordination distance R will be defined herein as the “virtual” energy storage gain. The maximum energy storage demand associated with the variance of the landscape hydropower potential is large in comparison to the available energy storage capacity within the European hydropower reservoirs, which is 183 TWh. Only for periods much shorter than a year can the available storage in reservoirs potentially have significant importance for the

regulation of energy production through hydropower. For comparison, the maximum energy storage demands based on the moving average time-series (Table 2, Fig. 3) were analysed. These estimations consider only the time period of the moving window; hence, they generally give a lower estimate of the energy storage demand compared to the spectral estimate. However, both estimates are on the same order of magnitude, which indicates that the spectral estimation of the energy storage demand provides reasonable results.

#### 4.3. Energy storage demand at hydropower plant locations

This study considers the hydropower potential at the 326 main river basins with hydropower plants and reservoirs covered in the GranD database. The system has an energy storage capacity of 81 TWh (Fig. 7, dotted line) that meets the maximum energy storage demand at the 1-year period regardless of coordination distances. For the periods 2–4.7 years, the results indicate that it is essential to select a sufficiently long coordination distance over the European continent to satisfy the energy balance  $(\partial E/\partial t - P_c)|_{\Omega} = 0$  at all times, while the system storage capacity is insufficient when all periods p to 14 years are considered even if  $R = 89$ . Moreover, when all periodicity areas take into account the ratio  $E_{max}|_{R=0}/E_{max}|_{R=89}=1.76$ , the maximum Virtual Energy Storage Gain (VESG) from spatial coordination is estimated to be  $E_{max}|_{R=0} - E_{max}|_{R=89}=140$  TWh (Fig. 7). For the selected hydropower system covered by GranD, the energy storage capacity is 81 TWh, which means that the spatial coordination of hydropower production over Europe can potentially represent nearly twice the energy storage gain as offered by the existing hydropower reservoirs. Furthermore, if one takes into consideration the 6.7–15% loss of the standard deviation in the spectral transform, the energy storage gain would be slightly higher. The virtual storage gain can in practice be limited by reservoir as well as transmission grid constraints, which will be further discussed in the next section.

## 5. Discussion

### 5.1. Virtual energy storage gain and energy droughts

The findings of this study suggest that the covariation of hydropower availability across larger regions can be intentionally utilized in production management to reduce the variance in hydropower

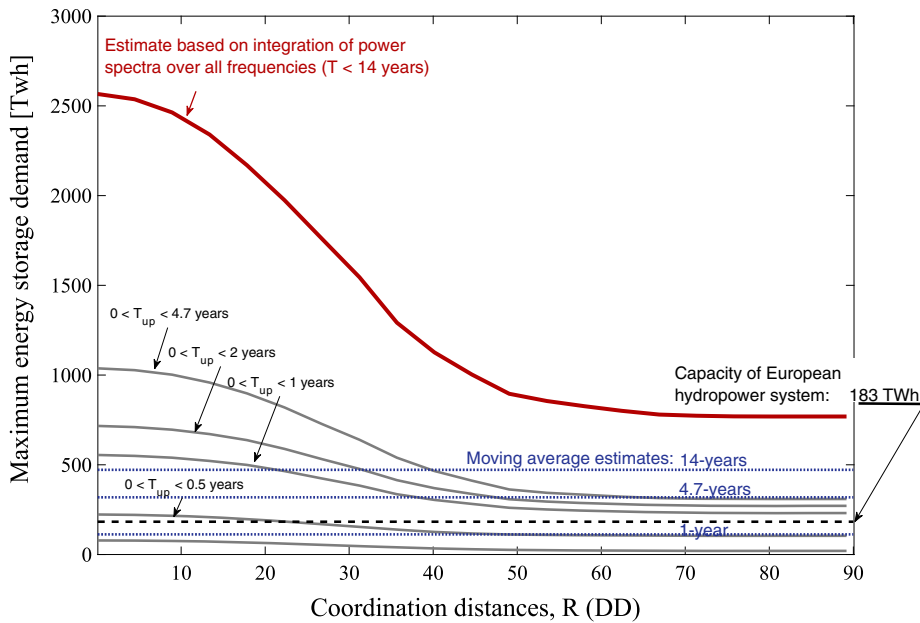


**Fig. 6.** Maximum energy storage demand associated with the temporal variance of the landscape hydropower potential as defined by the energy balance  $(\partial E / \partial t - P_c)_Q = 0$ . The red curve shows the decrease in energy storage demand due to the cumulative effect of all time periods up to 14 years. Grey curves show similar energy storage demand for different upper bounds of the time periods taken into consideration. The dashed line shows the estimated storage capacity of the European hydropower system (183,000 GWh). Dotted (blue) lines indicate the maximum energy storage demand based on the moving average time-series of the simultaneous landscape hydropower potential as a spatial average over all watersheds, as shown in Fig. 3. These results are summarized in Table 1.

production that results in a virtual energy storage gain. If such spatio-temporal coordination of the production is considered over a coordination distance  $R$ , the virtual energy storage gain goes from zero at  $R = 0$  DD to nearly twice the existing storage capacity of existing hydropower reservoirs covered by the GranD database at  $R = 89$  DD (3916–7031 km). The highest change in virtual storage gain is obtained

at distances from 1200 km up to 3000 km. A similar “virtual” storage gain can potentially be substantially greater when additional account is taken to different renewable energy sources with a high degree of internal availability correlation and, thus, should play a major role in regulating the intermittency of renewable energy production at the continental scale. As shown, this gain is particularly important as the

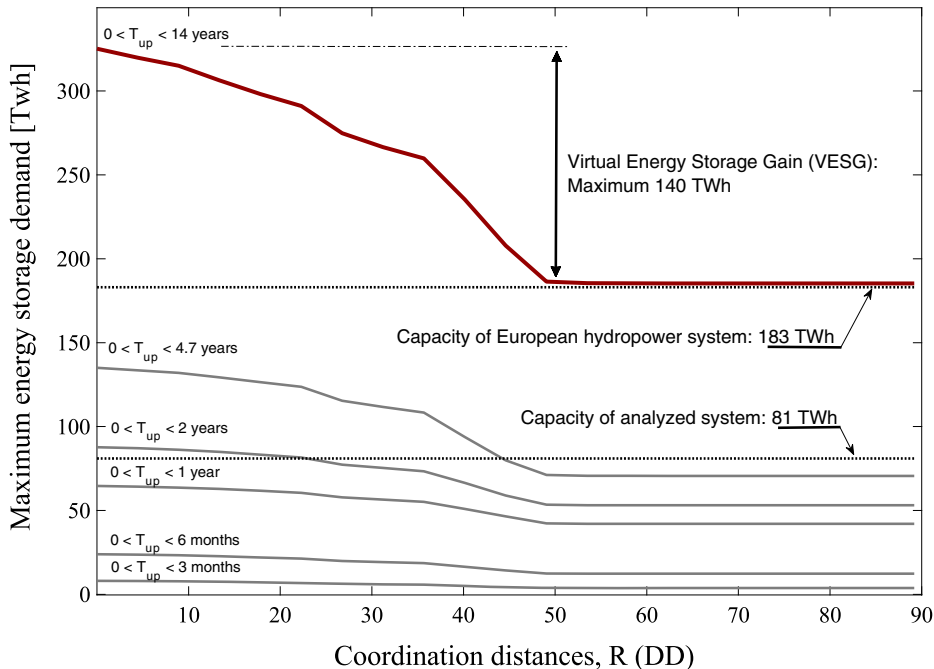


**Fig. 7.** Energy storage demand based on the hydropower plants covered by the GranD database. The lower, dotted line represents the energy storage capacity of the associated reservoirs, 81 TWh. The upper, dotted line is the entire energy storage capacity of the European hydropower system, 183 TWh.

time period under consideration increases, which is of high relevance due to the long-term climate fluctuations that have been observed in historical hydrometeorological data.

Failure to meet the balance of energy production, demand and storage can result, at high production availability, in a need to spill water at individual hydropower plants and, at low production availability, in a deficit between energy demand and production availability. The maximum energy storage demand that falls above the available energy storage capacity within the European hydropower system (Fig. 7) can be seen as an *energy-domain-specific drought*. This risk is prevalent at all periods longer than approximately five years but can be reduced by the spatio-temporal coordination of power production, which would then reduce the demand for a matching rest power  $\varepsilon$  that would be required to fulfil the energy balance. Such requirements might affect the export and import of energy, as well as other energy sources.

## 5.2. Implications for production management

Effectuating the virtual storage gain in practice would require new incentives in management models, and it can be limited by reservoir and transmission grid constraints. Generally, management models for large hydropower systems consider production objectives but indirectly represent reservoir storage levels [7]. Energy storage is an explicit part of the objective function in terms of the future value of the stored water, the “water value”. To account for an uncertain future in management, stochastic dual dynamic programming (SDDP) has been developed [42,43]. The single objective function generally includes economic “benefits” from production as well as penalty costs for not meeting certain target demands and violating operating constraints. In principle, virtual energy storage gain is not generally a production benefit in current management models (which account only for “real” storage) but could be seen as a specific target demand that can be accounted for in a single objective function approach to multi-reservoir management. Individual energy companies currently have resource management strategies that account for coordinated storage to some extent, but these strategies also involve other resting power capacities ( $\varepsilon$ ) in the form of energy export, energy import or the employment of other energy sources (Eq. (3)). Furthermore, the common economic incentives that prevail in energy markets tend to produce uniform management behaviour with a relatively high degree of correlation of hydropower production over the market region. Hence, a key challenge is to evaluate the virtual storage gain and introduce sound economic incentives for such benefit, i.e., identify mechanisms to pay for the benefit of reducing risks of energy droughts. One option to deal with seemingly incompatible benefits that cannot necessarily be evaluated in the same currency is to use dual objective assessments with Pareto curves defining the optimal combination of two objectives. Previously, such analysis has been performed for similar problems, such as hydropower production and environmental objectives [36,44], but could in principle also be applied to optimize the energy production over large domains.

## 5.3. Limitations and simplifications of analysis

The power spectral densities and variance of the landscape hydropower potential are calculated by using Eqs. (9) and (10). The last (second) sum on the right-hand side of Eq. (11) considers the correlation between all power time-series of the aggregated watersheds. However, the spectral estimate generally produces a somewhat lower estimate compared to that deduced in real-time space, which is because the spectral procedure “loses” some variance in numerical filtering (see Section 3.4). This behaviour implies that the spectral methods slightly underestimate the power, energy storage and possible gain from the spatial coordination of hydropower production.

The power spectrum approach developed within this paper defines necessary but not sufficient conditions for satisfying the energy balance in real-time space at all times. Phase spectra would be other essential criteria and constraints of the problem solution that would be important, e.g., for the distribution of the energy storage demand,  $E$ , but not necessarily for the variance of  $E$ .

The assumption of a single domain for energy storage and power availability capacity implies that all local restrictions of storage availability and production power capacities are neglected. Such simplification could in principle apply to a future technical solution, but currently, there are many examples of important restrictions in the production system, especially in, e.g., the capacity of hydropower plants at high flows and the transmission capacity of the electrical grid. The virtual energy storage gain implies a reduced hydro-energy storage demand in general, hence indirectly contributing to reduced constraints of the food-water-energy nexus from a wider system perspective. These constraints involve a large number of resource flows and interactions [45], which are affected by resource coordination and storage strategies for water and energy.

## 6. Conclusions

Several previous studies have found climate-driven periods of fluctuations in hydroclimatic variables over periods of 2, 3.6 and 8–11 years and, further, often with negative correlations between variables. This study confirms that hydropower production potential shows the highest variance at 1, 2 and 8–11 years and a minimum at approximately 3.6 years. By considering the spatio-temporal coordination of the production within a coordination distance, the variance in hydropower availability can be significantly reduced, which results in a *Virtual Energy Storage Gain* (VESG). This study assesses the spatio-temporal variance in hydropower production capacity of 3032 main river basins with effluence to the sea. Hydropower is naturally coordinated within these main river basins by using common reservoirs for energy storage, but significant virtual energy storage gain can also arise due to production coordination across these river basins. The spatio-temporal coordination of the hydropower production given by the GranD database in a domain covering large parts of Europe and the Middle East can potentially represent virtual energy storage twice that offered by existing reservoirs. The most significant gain from the spatial coordination of hydropower production is obtained at distances from 1200 km up to 3000 km, i.e., on the continental scale.

Virtual energy storage gain through spatio-temporal coordination might be important for avoiding failure of the energy balance at all times and locations, hence, for avoiding energy droughts as well as the spillage of water at hydropower plants. These findings reveal that for hydropower, one can expect that energy-domain specific drought occurs over time periods longer than two years and that the probability of failure increases significantly with the time period due to long-term climate-driven fluctuations in hydropower availability.

Hydropower and bioenergy are energy sources that can easily be stored and will therefore play key roles in a future renewable and intermittent energy system. The estimated two-fold increase in hydropower storage should greatly simplify the transition to a renewable energy system. In particular, due to the apparent intermittent nature and correlation between renewable energy sources, the variance of energy availability can be expected to be higher than that of a fossil and nuclear-based energy resource system. The higher power potential variance would imply a higher demand for energy storage but also offer a higher potential for virtual energy storage gain due to spatio-temporal coordination. We suggest further studies on such multiple renewable energy resource systems and on appropriate incentives in management models for recognizing virtual energy storage gain. One essential direction would be to account for a combined energy system with scenarios for solar and wind power as well as energy demand scenarios. It

would be relevant to utilize low internal correlation between renewable energies in the form of virtual energy storage. The identification of suitable locations for power plants will be key for utilizing both real storage and virtual storage as well as production capacity. Another direction would be market incentives for virtual energy storage on a system level, especially linked to long-term (from seasons to years and decades) forecasting of climate-driven energy fluctuations.

#### CRediT authorship contribution statement

**Anders Wörman:** Conceptualization, Data curation, Formal analysis, Funding acquisition, Investigation, Methodology, Project administration, Resources, Software, Supervision, Validation, Visualization, Writing - original draft, Writing - review & editing. **Cintia Bertacchi Uvo:** Funding acquisition, Investigation, Resources, Validation, Visualization, Writing - review & editing. **Luigia Brandimarte:** Data curation, Investigation, Writing - review & editing. **Stefan Busse:** Funding acquisition, Supervision, Writing - review & editing. **Louise Crochemore:** Data curation, Investigation, Resources, Writing - review & editing. **Marc Girons Lopez:** Data curation, Investigation, Resources, Writing - review & editing. **Shuang Hao:** Conceptualization. **Ilias Pechlivanidis:** Data curation, Funding acquisition, Investigation, Project administration, Resources, Supervision, Validation, Writing -

review & editing. **Joakim Rimi:** Conceptualization, Formal analysis, Supervision, Writing - review & editing.

#### Declaration of Competing Interest

The authors declare that they have no known competing financial interests or personal relationships that could have appeared to influence the work reported in this paper.

#### Acknowledgements

This study was financially supported by the project named “Long-term forecasts of wind and hydropower supply in a fluctuating climate – Importance for production planning and investments in energy storage and power transmission” granted by the Swedish Energy Agency under grant agreement No. 46412-1. Funding was also provided through the Swedish strategic research programme StandUp for Energy.

The HYPE model code is available from the HYPEweb portal (<http://hypeweb.smhi.se/model-water/>). Historical modelled data obtained through E-HYPE are openly available on the HYPEweb portal (<https://hypeweb.smhi.se/explore-water/historical-data/europe-long-term-means/>).

#### Appendix A. Potential of the annual mean renewable energy production in the world

**Hydropower:** The current production in the world is 3894 TWh/y [46]. According to the IEA, there is a potential to expand hydropower by a factor of  $\sim 3$ , but it depends significantly on different environmental and economic constraints. A recent study suggests that the gross theoretical hydropower potential is approximately 52,000 TWh/y [4]. Other sources provide estimates of the technical potential production capacity of approximately 14,500 TWh/y [45,48].

**Bioenergy:** In 2009, bioenergy use (production) was approximately 10,500 TWh/y, including traditional wood, which is the dominant part [3,48]. Currently, the IEA [46] reports the use of traditional wood (biomass) corresponding to 9001 TWh/y and 5742 TWh/y in the form of electricity production, which makes a total production of 14,743 TWh/y. The IEA proposed a scenario for bioenergy development until 2040 that would correspond to approximately 30,000 TWh/y. The production potential is limited only by the technology used and the natural circumstances, and the sustainable potential has been estimated to be in the range of 55,600 TWh/y – 417,000 TWh/y. These estimates consider a range of environmental and social constraints to guarantee sustainable feedstock production.

**Solar power (PV):** The global average solar radiation that is absorbed by the surface of the Earth corresponds to approximately 170 W/m<sup>2</sup> [5]. Given a solar cell efficiency of 16% and a complete coverage of all the land on Earth (land area is  $149 \cdot 10^{12} \text{ m}^2$ ) yields a maximum potential solar energy production of 3,550,000 TWh/y. This potential is highly limited by technical and economic constraints as well as the prioritization of land use.

**Wind power:** The US Department of Energy has presented a scenario for wind power production where 35% of the total electricity consumption is produced by wind power by 2050 [49]. If this scenario is projected on world electricity production, 23,950 TWh/y (Global Energy Statistical Yearbook 2016), there would be a foreseeable wind power potential of 8380 TWh/y. However, the actual potential is much higher.

**Marine power:** The current scenarios for marine power indicate a minor importance for the total energy production of 92 TWh/y by 2040 according to IEA [46].

**Geothermal:** The current scenarios for marine power indicate a minor importance for the total energy production, 548 TWh/y by 2040 according to IEA [46]. The flux of geothermal energy due to the radioactivity of the interior of the Earth is approximately 0.1 W/m<sup>2</sup>, which gives a maximum potential on land of 133,526 TWh/y, but it has limited technical availability.

#### Energy demand

By 2050, the global energy demand is estimated to grow from the current level of 160,000 TWh/y to 208,000 TWh/y [46]

#### Average water availability

Hoekstra and Mekonnen [50] estimated the average water footprint due to domestic, industrial and agricultural production to be  $9087 \times 10^9 \text{ m}^3/\text{y}$ , or approximately 7.6% of the estimated effective worldwide runoff (UN statistics 2016).

#### Appendix B. Power spectra of the hydropower availability in different locations in Europe

Normalized power spectra of the landscape hydropower potential were defined as the power spectral densities divided by the total variance and calculated for square areas with side lengths of 1.5 DD (red rectangle in the figure) for different central points in Europe. This demonstration is by no means exhaustive but shows to some extent systematic variation in the power spectral diagram over Europe. These differences in the spatio-temporal variation in the hydropower potential have implications for appropriate resource planning, especially for spatio-temporal coordination of resources. Dark points show the coordinates of 1377 hydropower stations of the GranD database, and coloured areas show the 3.032 main watersheds used in the E-HYPE runoff simulations (see Fig. A1).

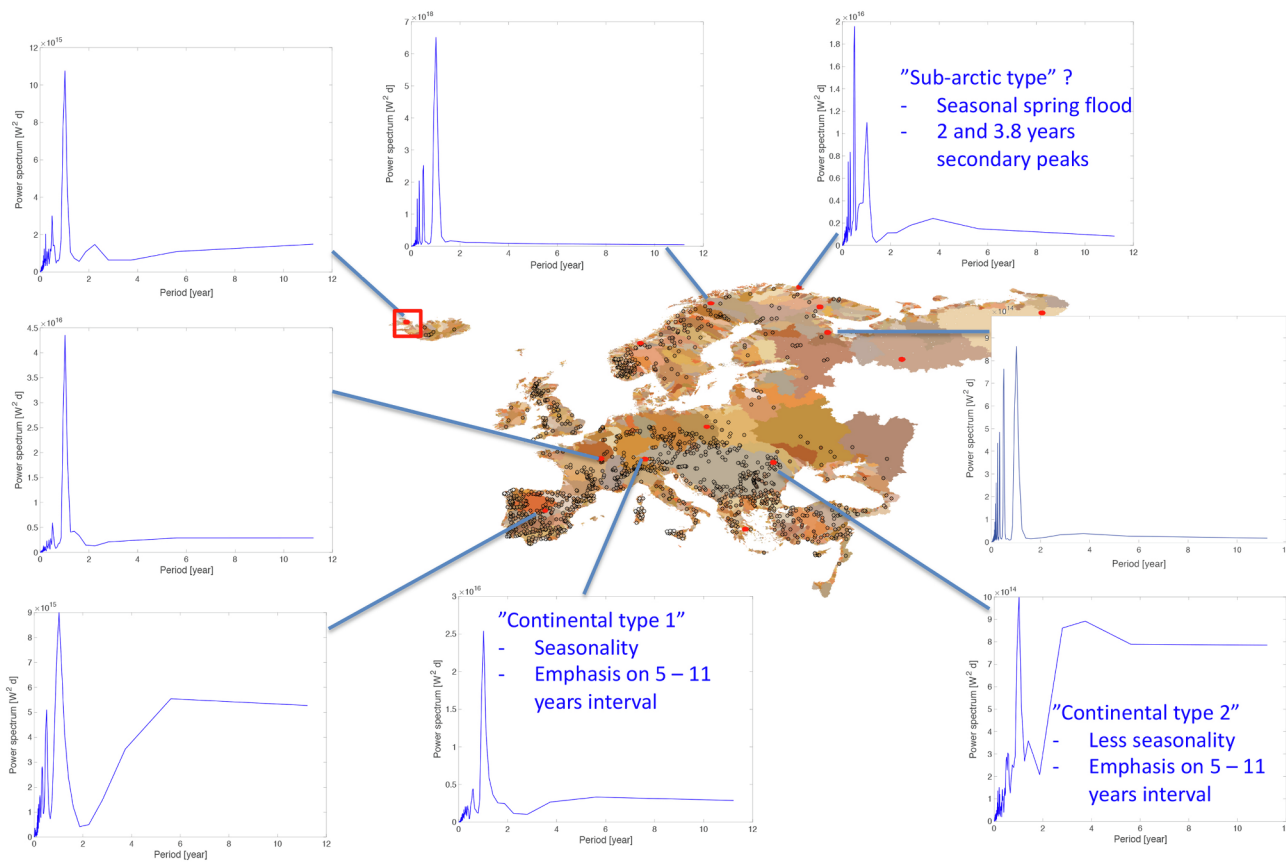


**Fig. A1.** Power spectra of the hydropower availability in different locations in Europe.

## References

- [1] Engeland K, Borga M, Creutin JD, François B, Ramos MH, Vidal JP. Space-time variability of climate variables and intermittent renewable electricity production – a review. *Renew Sustain Energy Rev* 2017;79(2017):600–17.
- [2] Kang J-N, Wei Y-M, Liu L-C, Han R, Yu B-Y, Wang JW. Energy systems for climate change mitigation: A systematic review. *Appl Energy* 2020;263:11460.
- [3] Bauen A, Berndes G, Junginger M. Bioenergy – A sustainable and reliable energy source: A review of status and prospects. *IEA Bioenergy: ExCo 2009*;2009:06.
- [4] Hoes OAC, Meijer LJ, van der Ent RJ, van de Giesen NC. Systematic high-resolution assessment of global hydropower potential. *PLOS One*; 2017. doi: 10.1371/journal.pone.0171844.
- [5] Trenberth KE, Fasullo JT, Kiehl J. Earth's global energy budget. *Bull Am Meteor Soc* 2009;90:311–23.
- [6] Teegavarapu RSV, Simonovic SP. Short-term operation model for coupled hydropower reservoirs. *J Water Resour Plan Manag Asce* 2000;126:98–106. [https://doi.org/10.1061/\(ASCE\)0733-9496\(2000\)126:2\(98\)](https://doi.org/10.1061/(ASCE)0733-9496(2000)126:2(98)).
- [7] Labadie JW. Optimal operation of multireservoir systems: state-of-the-art review. *J Water Resour Plan Manag Asce* 2004;130:93–111. [https://doi.org/10.1061/\(ASCE\)0733-9496\(2004\)130:2\(93\)](https://doi.org/10.1061/(ASCE)0733-9496(2004)130:2(93)).
- [8] Contreras E, Herrero J, Crochemore L, Pechlivanidis I, Photiadou C, Aguilar C, et al. Advances in the definition of needs and specifications for a climate service tool aimed at small hydropower plants' operation and management. *Energies* 2020;13:1827. <https://doi.org/10.3390/en13071827>.
- [9] Gjorgiev B, Sansavini G. Electrical power generation under policy constrained water-energy nexus. *Appl Energy* 2018;210(2018):568–79.
- [10] Giuliani M, Crochemore L, Pechlivanidis I, Castelletti A. From skill to value: isolating the influence of end-user behaviour on seasonal forecast assessment. *Hydrol Earth Syst Sci Discuss* 2020. <https://doi.org/10.5194/hess-2019-659>, in review.
- [11] Raynaud D, Hingray B, François B, Creutin JD. Energy droughts from variable renewable energy sources in European climates. *Renew Energy* 2018;125:578–89.
- [12] François B, Borga M, Anquetin S, Creutin JD, Engeland K, Favre AC, et al. Integrating hydropower and intermittent climate-related renewable energies: a call for hydrology. *Hydrol Process* 2014;28:5465–8. <https://doi.org/10.1002/hyp.10274>.
- [13] Kingston DG, McGregor GR, Hannah DM, Lawler DM. River flow teleconnections across the northern North Atlantic region. *Geophys Res Lett* 2006;33(14).
- [14] Kingston DG, Hannah DM, Lawler DM, McGregor GR. Climate–river flow relationships across montane and lowland environments in northern Europe. *Hydrol Process: Int J* 2009;23(7):985–96.
- [15] Trigo RM, Pozo-Vazquez D, Osborn TJ, Castro-Díez Y, Gamiz-Fortis S, Esteban-Parra MJ. North Atlantic oscillation influence on precipitation, river flow and water resources in the Iberian peninsula. *Int J Climatol* 2004;24(8):925–44. <https://doi.org/10.1002/joc.1048>.
- [16] Brandimarte L, Di Baldassarre G, Bruni G, D'Odorico P, Montanari A. Relation between the North-Atlantic Oscillation and hydroclimatic conditions in Mediterranean areas. *Water Resour Manage* 2011;2011(25):1269–79. <https://doi.org/10.1007/s11269-010-9742-5>.
- [17] Bartolini E, Claps P, D'Odorico P. Interannual variability of winter precipitation in the European Alps: relations with the North Atlantic Oscillation. *Hydrol Earth Syst Sci* 2009;13(1):17–25. <https://doi.org/10.5194/hess-13-17-2009>.
- [18] Ely CR, Brayshaw DJ, Methven J, Cox J, Pearce O. Implications of the North Atlantic Oscillation for a UK–Norway Renewable powersystem. *Energy Policy* 2013;62(2013):1420–7.
- [19] Wörman A, Lindström G, Riml J. The power of runoff. *J Hydrol* 2017;548(2017):784–93. <https://doi.org/10.1016/j.jhydrol.2017.03.041>.
- [20] Wallace JM, Gutzler DS. Teleconnections in the geopotential height field during the Northern Hemisphere winter. *Mon Weather Rev* 1981;109(4):784–812.
- [21] Uvo CB. Analysis and Regionalization of Northern European Winter Precipitation based on its relationship with the North Atlantic Oscillation. *Int J Climatol* 2003;23:1185–94.
- [22] Yuan F, Berndtsson R, Bertacchi Uvo C. Hydro climatic trend and periodicity for the source region of the Yellow River. *J Hydrol Eng* 2015;20(10). 05015003.
- [23] Herran DS, Tachiiri K, Matsumoto K. Global energy system transformations in mitigation scenarios considering climate uncertainties. *Appl Energy* 2019;243(2019):119–31.
- [24] Kundzewicz ZW, Kanae S, Seneviratne SI, Handmer J, Nicholls N, Peduzzi P, et al. Flood risk and climate change: global and regional perspectives. *Hydrol Sci J* 2014;59(1). <https://doi.org/10.1080/02626667.2013.857411>.
- [25] Lamb PJ, Peppler RA. West Africa. In: Glantz MH, Katz RW, Nicholls N, editors. *Teleconnections linking worldwide climate anomalies: scientific basis and societal impact*. London: Cambridge University Press; 1991. p. 121–89, Chapt. 5.
- [26] Meddi MM, Assani AA, Meddi H. Temporal variability of annual rainfall in the macta and tafna catchments, Northwestern Algeria. *Water Resour Manage* 2010;24:3817–33. <https://doi.org/10.1007/s11269-010-9635-7>.
- [27] Foster K. Hydrological seasonal forecasting. Doctoral Dissertation. Division of Water Resources Engineering, Lund University; 2019. ISBN: 978-91-7623-986-5.
- [28] Uvo CB, Foster K, Olsson J. The spatio-temporal influence of atmospheric teleconnection patterns on hydrology in Sweden. *Climate Dynamics*; 2020 [under revision].
- [29] Lindström G, Pers C, Rosberg J, Strömqvist J, Arheimer B. Development and testing

- of the HYPE (Hydrological Predictions for the Environment) water quality model for different spatial scales. *Hydrol Res* 2010;41(3–4):295. <https://doi.org/10.2166/nh.2010.007>.
- [30] Donnelly C, Andersson JCM, Arheimer B. Using flow signatures and catchment similarities to evaluate the E-HYPE multi-basin model across Europe. *Hydrol Sci J* 2016;61(2):255–73. <https://doi.org/10.1080/02626667.2015.1027710>.
- [31] Hundecha Y, Arheimer B, Donnelly C, Pechlivanidis I. A regional parameter estimation scheme for a pan-European multi-basin model. *J Hydrol: Reg Stud* 2016;6(Supplement C):90–111. <https://doi.org/10.1016/j.ejrh.2016.04.002>.
- [32] Berg P, Donnelly C, Gustafsson D. Near-real-time adjusted reanalysis forcing data for hydrology. *Hydrol Earth Syst Sci* 2018;22(2):989–1000. <https://doi.org/10.5194/hess-22-989-2018>.
- [33] Lehner B, Reidy Liermann C, Revenga C, Vörösmarty C, Fekete B, Crouzet P, et al. High-resolution mapping of the world's reservoirs and dams for sustainable river-flow management. *Front Ecol Environ* 2011;9(9):494–502.
- [34] Beames et al. Global Reservoir and dam (GRanD) Database: technical documentation – version 1.3. February 2019; 2019. <http://globaldamwatch.org>.
- [35] ICOLD. World Register of Dams; 2019. [https://www.icold-cigb.org/GB/world\\_register/world\\_register\\_of\\_dams.asp](https://www.icold-cigb.org/GB/world_register/world_register_of_dams.asp).
- [36] Zmijewski N, Wörman A. Hydrograph variances over different timescales in hydropower production networks. *Water Resour Res* 2016;52:5829–46. <https://doi.org/10.1002/2015WR017775>.
- [37] Tabony RC. A principal component and spectral analysis of European rainfall. *Int J Clim* 1981;1(3):283–94.
- [38] Moron V, Vautard R, Ghil M. Trends, Interdecadal annual oscillations in Global Sea-surface temperatures. *Clim. Dyn.* 1998;14:545–69.
- [39] Movahed MS, Jafari GR, Ghasemi F, Rahvar S, Tabar MRR. Multifractal detrended fluctuation analysis of sunspot time series. *J. Stat. Mech.* 2006;2006:P02003. <https://doi.org/10.1088/1742-5468/2006/02/P02003>.
- [40] Pekárová P, Miklánek P, Pekár J. Spatial and temporal runoff oscillation analysis of the main rivers of the world during the 19th–20th centuries. *J. Hydrol.* 2003;274:62–79.
- [41] Karagiannidis AF, Bloutsos AA, Maheras P, Sachamanoglou Ch. Some statistical characteristics of precipitation in Europe. *Theor Appl Climatol* 2007;91:193–204. <https://doi.org/10.1007/s00704-007-0303-7>.
- [42] Tilmant A, Pinte D, Goor Q. Assessing marginal water values in multipurpose multireservoir systems via stochastic programming. *Water Resour Res* 2008;44:W12431. <https://doi.org/10.1029/2008WR007024>.
- [43] Goor Q, Kelmar R, Tilmant A. Optimal multipurpose-multireservoir operation model with variable productivity of hydropower plants. *J Water Resour Plann Manage* 2011;137(3):258–67. [https://doi.org/10.1061/\(ASCE\)WR.1943-5452.0000117](https://doi.org/10.1061/(ASCE)WR.1943-5452.0000117).
- [44] Zmijewski N, Wörman A. Trade-offs between phosphorous discharge and hydropower production using reservoir regulation. *J Water Resour Plann Manage* 2017;143(9):04017052. Doi: 10.1061/(ASCE)WR.1943-5452.00000809.
- [45] Bazilian M, Rogner H, Howells M, Hermann S, Arent D, Gielen D, et al. Considering the energy, water and food nexus: Towards an integrated modelling approach. *Energy Policy* 2011;39(2011):7896–906.
- [46] IEA. World Energy Outlook 2016. OECD/IEA, 2016 International Energy Agency; 2016.
- [47] Lane T. Lead author for world energy council's report on world energy resources; 2015. ISBN: 978 0 946121 41 0.
- [48] Kumar A, Schei T, Ahenkorah A, Caceres Rodriguez R, Devernay J-M, Freitas M et al. Hydropower. In: Edenhofer O, Pichs-Madruga R, Sokona Y, Seyboth K, Matschoss P, Kadner S et al., editors, IPCC special report on renewable energy sources and climate change mitigation; 2011.
- [49] US DOE. Wind Vision: A New Era for Wind Power in the United States; 2015. Available electronically at <http://www.osti.gov/scitech>.
- [50] Hoekstra AY, Mekonnen MM. The water footprint of humanity. *PNAS* 2011;3232–7. <https://doi.org/10.1073/pnas.1109936109>.